STUDIES ON NATURAL VIBRATIONS OF A LATHE-BED WITH HYPERBOLOID RIBBING

By

C. S. NAGARAJ

DEPARTMENT OF MECHANICAL ENGINEERING

INDIAN INSTITUTE OF TECHNOLOGY KANPUR

JANUARY, 1974

TO

My wife Nagalakshmi

My daughter Ramä

My son Vijayaraj

whose sacrifice to enable me to complete the task is too great to recompense

and

Friends

who retrieved me from the abyss of physical calamity that had engulfed me.

ACKNOWLEDGEMENTS

I am immeasurably indebted to the Government of Gujarat for its magnanimity of providing me an opportunity with all facilities, to prosecute post-graduate studies.

I am very grateful to Dr. G.S. Kainth, Department of Mechanical Engineering for suggesting the problem, keen interest shown in the work, enthusiastic guidance and kindness shown to me at all times.

I sincerely thank Dr. N.G.R. Iyengar, Department of Aeronautical Engineering for his very valuable suggestions at different stages of the work.

I am indebted to Mr. G.V. Narayan and Mr. M. Hariharan of Department of Civil Engineering for their invaluable help without which this work could not have been completed in time.

I am thankful to Mr. Uma Raman Pandey for his excellent typing of the manuscript.

C.S. NAGARAJ

CERTIFICATE

Certified that this work has been carried out under my supervision and that this has not been submitted elsewhere for a degree.

G.S. KAINTH 8/1/74
Assistant Professor
Department of Mechanical Engineering
I.I.T.Kanpur

SYNOPSIS

C.S. NAGARAJ
M.TECH.(MECH.)
INDIAN INSTITUTE OF TECHNOLOGY
KANPUR
JAN., 1974

STUDIES ON NATURAL VIBRATIONS
OF A LATHE-BED WITH HYPERBOLOID RIBBING

Chatter is an undesirable phenomenon in machine tool operation. One of the factors that have a bearing on chatter is the natural frequency of the vibrating system.

In the present work a HMT Lathe-bed SK-62-206-5, has been analyzed to predict the natural frequencies and modes of vibration using lumped-mass method. Two types of idealizations are considered. Effect of variation in wall thickness 't' and wall depth 'd' on natural frequencies is studied.

A general computer programme is developed with the aid of which lathe-bed with different types of ribbings can also be analyzed in addition to the study of effect of variation in structural parameters on the natural frequency.

TABLE OF CONTENTS

CHAPTER I

INTRODUCTION

When a machine tool is utilized to cut metal it may experience three types of vibrations namely free, forced and self-excited vibrations. Free vibrations arising due to shock and forced vibrations arising due to unbalanced rotating parts etc. can be eliminated when the cause is known. Self-excited vibrations arise due to **variation** of cutting conditions such as depth of cut and cutting speed. The variation in cutting conditions generates a change dp in cutting force p. Depending upon the nature of dp, the resulting vibrations either grow or decay. Growth of vibrations leads to unstable cutting conditions and decay leads to steady-state cutting conditions. The self-excited vibrations are referred to as "chatter" in metal cutting. The source of self-exciting energy is in the cutting process itself.

The basic diagram of the process of self-excited vibrations in metal cutting is shown in Fig. 1. It is a

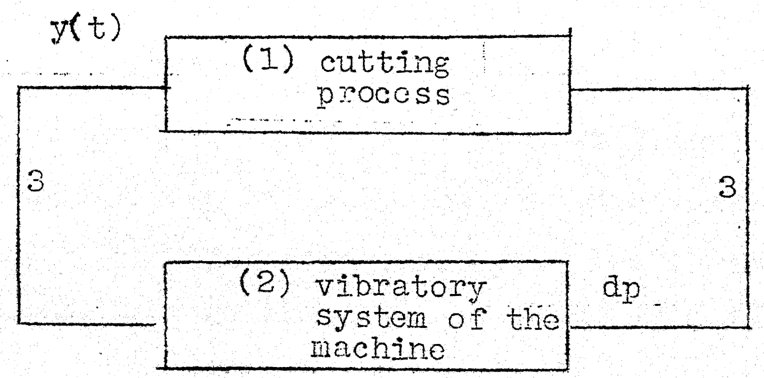

Fig. 1 : Basic diagram of chatter

closed-loop system and has three elements. Element (1) is the cutting process. Element (2) is the vibratory system of the machine. Element (3) is the mutual directional orientation of element (1) and element (2). Vibration y(t) between tool and work piece influences the cutting process (i.e. part (1)) so as to cause a variation dp of the cutting force p. 'dp', acting on the vibratory system of the machine creates again vibration y(t). Limit conditions for stable machining are changed if the mutual directional orientation of Element (1) and Element (2) is changed.

Chatter is a violent vibration between the tool and the work-piece. Chatter is detrimental to surface finish, tool life and production rate. Many chatter theories have been propounded[1,2,3,4]. The process of chatter has been studied with the aim of creating firstly rules by means of which the choice of cutting conditions can be made and secondly, rules for the design of machine tools with higher stability.

Machine tool structure has significant effect on the stability of the cutting process. The dynamic behavior of the machine tool structure is of immense importance because the cutting process will remain free of disturbance if the stiffness between the work and the tool and the stiffness in the drive are infinitely great. Cutting process is disturbed if the steady state

relative motion of the tool is altered. Steady state relative motion of the tool is altered if the tool deflects or if a twist occurs in the transmission train or on account of some similar cause.

The variation dp in cutting force p ('dp' is also called dynamic cutting force element) acts on the machine structure and forces the structure into vibration. This effects a change in the relative position of the cutting edge which in turn leads to a change in 'dp'. The disturbance forces the structure to vibrate in one or more of its natural modes of vibration. The natural mode determines the relative motion of the cutting edge with reference to the work and is also partly responsible for deciding the form and characteristic of the dynamic cutting force element 'dp'.

The ideal machine tool design warrants freedom from chatter. The stability of cutting process is dependent on both natural and chatter frequencies in addition to other parameters [1]. Hence, the knowledge of natural frequencies and normal modes of vibration of the machine tool structure is essential to an understanding of the dynamic response of a structure under any kind of excitation.

Since 1963, research workers have started working towards the prediction of dynamic characteristics by computers[5,6,7]. Hinduja and Cowley[8] have

stated that 'Finite-element Method' is superior to 'beam-like element approach'. One of the limitations of the beam-like element approach, according to them, is that "It is difficult to define the equivalent beam characteristics of machine tool structural elements, particularly those of non-slender form and with internal ribbing and apertures etc.". Their conclusion is that the superior technique of finite element method involves high computating costs and this is the limitation for its use.

Despite the claim of superiority of 'Finite-element Method' and the limitations of the 'Beam-like element approach with lumped masses', the latter lends itself to a substantial simplification in the mathematical problems involved in determining the static and dynamic stiffness characteristics of a structure.

In view of the above observation, beam-like elements with lumped-masses are used to idealise the H.M.T. lathe-bed structure (SK-62-206-5) for predicting natural frequencies and modes of vibration. A computer programme is developed to compute the results. The design of the lathe-bed is analyzed with two different types of idealization. For the original design, the effects of variation of the structural parameters, namely thickness of the main walls and their depth, are studied.

CHAPTER II

ANALYTICAL DETERMINATION OF NATURAL FREQUENCIES AND NATURAL MODES OF VIBRATION

2.1 INTRODUCTION

In the absence of exciting force and damping neglected, the equation of motion for multi-degree lumped-mass system may be written as

$$[M]_D \{\ddot{y}\} + [K]\{y\} = 0 \qquad (2.1.1)$$

where $[K]$ and $[M]_D$ are stiffness and mass matrices respectively and $\{y\}, \{\ddot{y}\}$ are the generalized co-ordinates and their second derivatives respectively. To find the natural frequencies and modes of vibration, therefore, it is necessary to obtain the structure stiffness matrix $[K]$ and the structure mass matrix $[M]_D$. The H.M.T. lathe-bed structure, details of which are shown in the drawings (Appendix II), is idealized as shown in Fig.2. For each element, element-stiffness matrix and element-mass matrix in element-oriented axes are obtained. Each one of these matrices is transformed to chosen global coordinates. Assembly of these transformed matrices produces the matrices $[K]$ and $[M]_D$.

Inserting these values in eqn.(2.1.1) and reducing it to an eigen value problem, the eigen values are found by power method given in reference (14). The eigen values thus found give the reciprocal of the square of the natural frequencies whereas eigen vector associated with each eigen value gives the mode shape.

Truly distributed mass systems have an infinite number of degrees of freedom. For practical purposes it is sufficient to deal with limited number of degrees of freedom, which can be represented by a lumped-mass-spring system. Hence the lumped-mass method is used for the present analysis.

2.2 IDEALIZATION OF THE STRUCTURE

A line diagram (Fig.2) shows the portion of the lathe-bed structure (Appendix II) between the bolted ends. The front-wall and the rear-wall are each divided into 7 elements. The ribs joining the front and rear walls are separated into 14 elements. In all there are 28 elements and 22 joints. The joints are also known as nodes. Nodes 1, 2, 21 and 22 are fully restrained. In case of three-dimensional motion, there are six degrees of freedom at each node. As there are 18 free nodes, the number of degrees of freedom in this case is 108. The nodes are so numbered that the band-width of resulting structure stiffness matrix is as narrow as possible. The elements are numbered row-wise.

It is assumed that the lengths of the elements-length along the centroidal axis of the element- lie in a plane. The ends of the bed are treated as rigidly fixed. The system of one of the intermediate ribbings is shown in Fig. 3. This ribbing is of inverted 'U'

IDEALIZED STRUCTURE

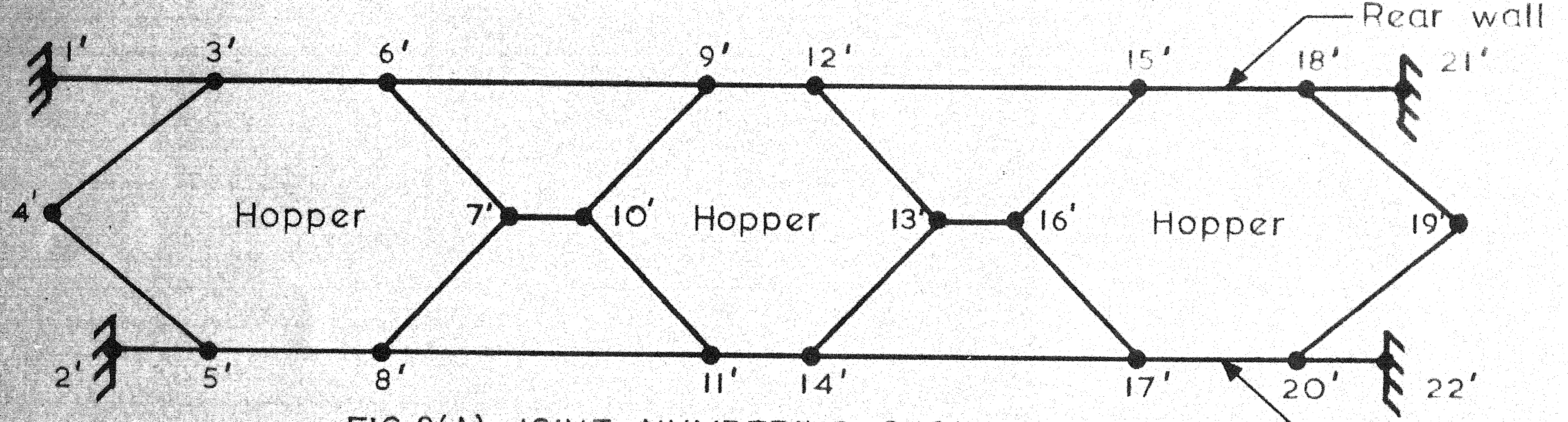

FIG.2(A) JOINT NUMBERING SEQUENCE

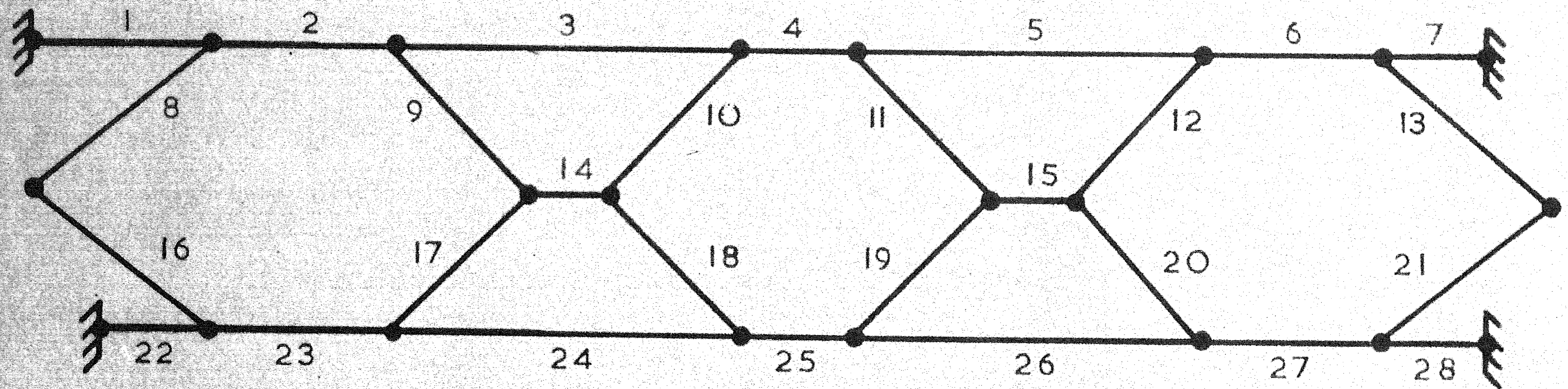

FIG.2(B) ELEMENT NUMBERING SEQUENCE

No. of elements 28
No. of joints 22 (primed numbers)
No. of restrained joints 4
No. of degrees of freedom 108

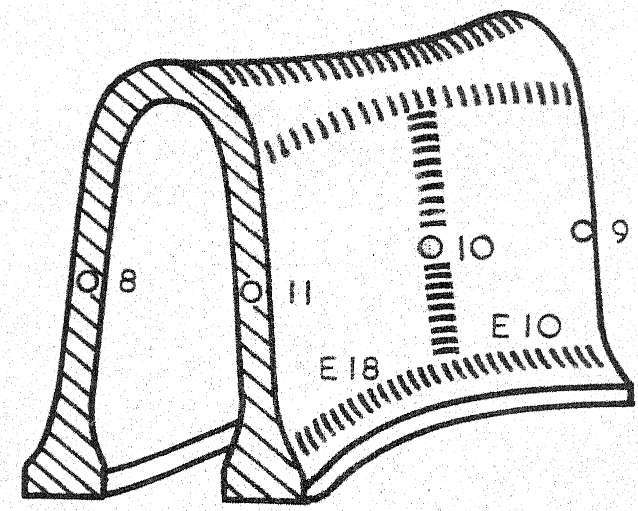

FIG. 3 INTERMEDIATE RIBBING

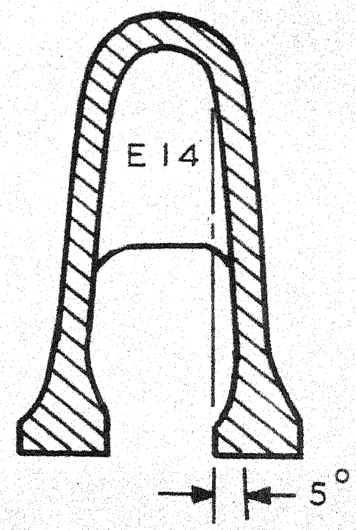

FIG. 4 CROSS-SECTION OF INTERMIDIATE RIBBING AT THE CENTRE

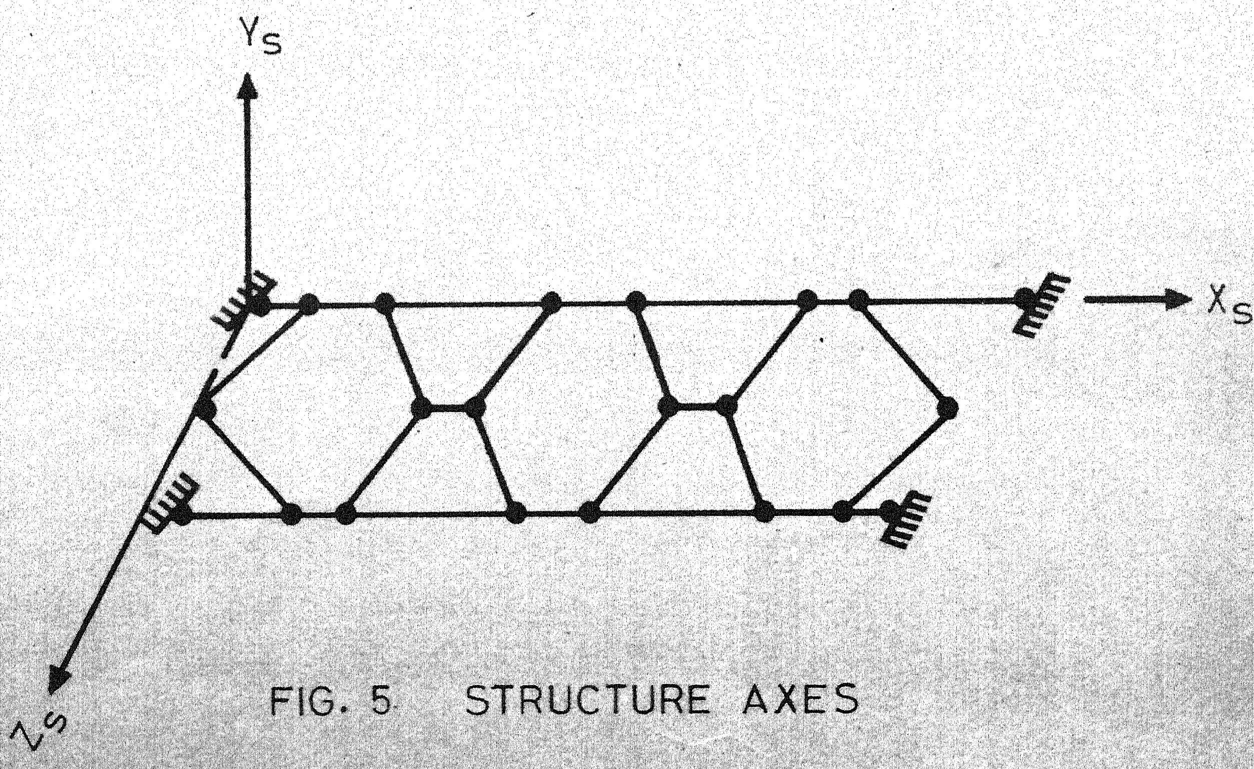

FIG. 5 STRUCTURE AXES

shape. Its limbs are hyperbolic in shape when seen in the plan view. The entire ribbing is idealized as forming 5 elements (9, 10, 14, 17, 18). A vertical cross-section of the ribbing at the centre is shown in Fig. 4, showing the stiffner element 14 and the inclination of the limbs to the vertical. This inclination being only 5° is ignored. The guide strips, bolted on to the top of the front and rear walls, are considered integral with the walls. The curved portions in the cross-section are approximated by straight lines.

The structure axes are chosen as shown in Fig. 5. The element axis x_e coincides with the centroidal axis of the element. In the case of main wall elements 1 to 7 and 22 to 28 x_e-axis coincides with the structure axis x_s. The orientation of ribbings is shown in Fig.2.

2.3 ELEMENT STIFFNESS MATRIX

The element stiffnesses for the restrained element shown in Fig. 6 are the actions exerted on the element by the restraints when unit displacements (translations and rotations) are imposed at each end of the element. The values of these restraints are given in reference (9). The unit displacements are considered to be induced one at a time while all other end-displacements are retained at zero and they are assumed to be positive in x_e, y_e and z_e directions. Thus the positive senses of the three translations

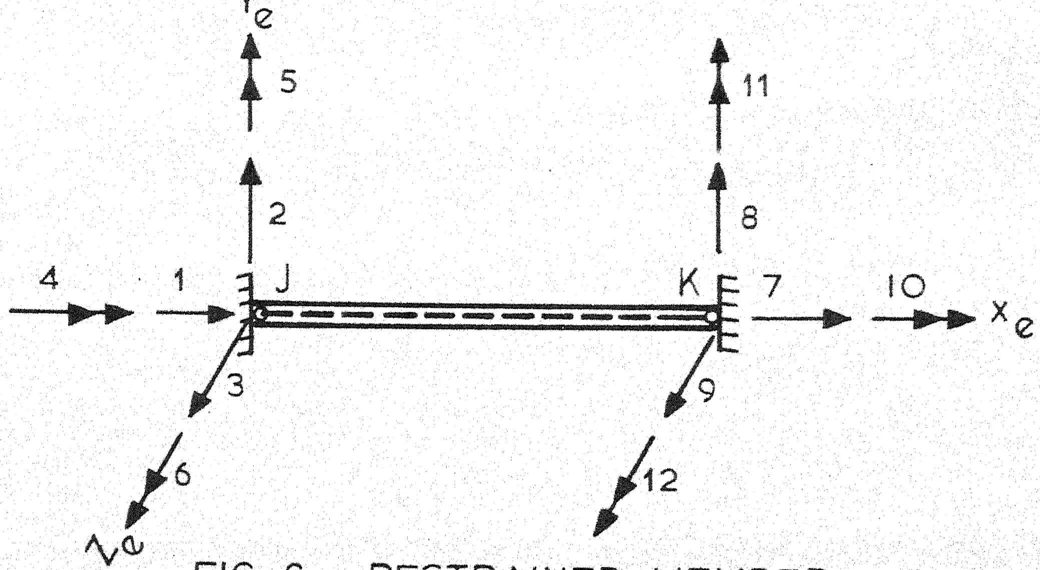

FIG. 6 RESTRAINED MEMBER

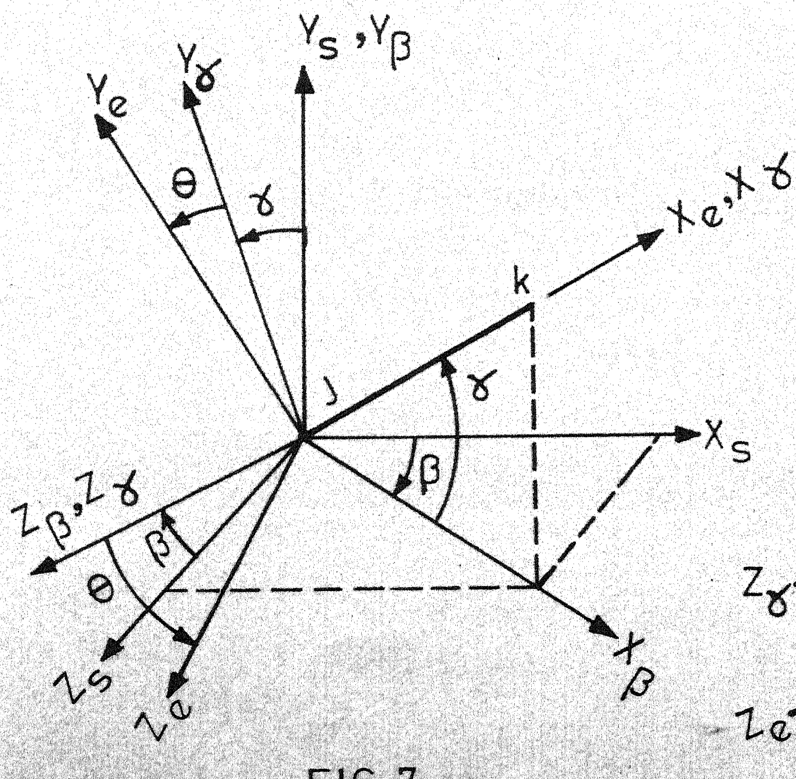

FIG. 7
ROTATION OF AXES FOR A SPACE FRAME MEMBER

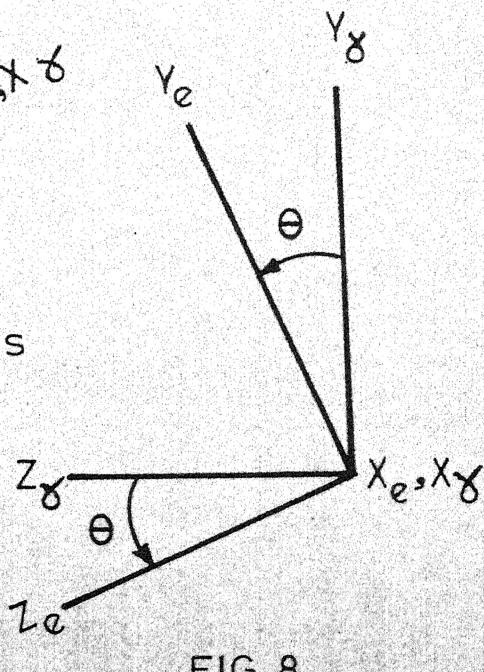

FIG. 8
ROTATION ABOUT X_e AXIS

and three rotations at each end of the element are indicated in Fig. 6. The single headed arrows denote translations and double headed ones the rotations.

There are twelve displacements in all and the resulting stiffness matrix for the element is (12x12). The derivation of the element stiffness matrix is given in reference (9). The stiffness matrix derived, is for a beam-element. It is utilized in the analysis as the beam-characteristic dominates in the given structure. As the depth to length ratio is fairly high (about 0.18), the shear deformation cannot be neglected. Therefore the stiffness-matrix for the beam-element derived in reference (10) which takes into account shear deformation is adapted and is given in Table 1.

2.4 ELEMENT MASS MATRIX

During the free-harmonic vibration of the structure, inertia forces will exist throughout the whole structure[4]. The structural mass may be represented by discrete mass points. The masses are lumped at the nodes. The inertia forces may be represented at all such points by equation of the form:

$$P_m \text{ Sin } w_n t = M_m D_m w_n^2 \text{ Sin } w_n t \qquad (2.4.1)$$

where,

$P_m \text{ Sin } w_n t$ = the inertia force acting at mass point 'm'

TABLE 1

$$
\begin{array}{cccccccccccc}
\frac{EA}{L} & & & & & & & & & \text{Symmetric} & & \\
0 & \frac{12EI_z}{L^3(1+\phi_y)} & & & & & & & & & & \\
0 & 0 & \frac{12EI_y}{L^3(1+\phi_z)} & & & & & & & & & \\
0 & 0 & 0 & \frac{GJ}{L} & & & & & & & & \\
0 & 0 & \frac{-6EI_y}{L^2(1+\phi_z)} & 0 & \frac{(4+\phi_z)EI_y}{L(1+\phi_z)} & & & & & & & \\
0 & \frac{6EI_z}{L^2(1+\phi_y)} & 0 & 0 & 0 & \frac{(4+\phi_y)EI_z}{L(1+\phi_y)} & & & & & & \\
\frac{-EA}{L} & 0 & 0 & 0 & 0 & 0 & \frac{AE}{L} & & & & & \\
0 & \frac{-12EI_z}{L^3(1+\phi_y)} & 0 & 0 & 0 & \frac{-6EI_z}{L^2(1+\phi_y)} & 0 & \frac{12EI_z}{L^3(1+\phi_y)} & & & & \\
0 & 0 & \frac{-12EI_y}{L^3(1+\phi_z)} & 0 & \frac{6EI_y}{L^2(1+\phi_z)} & 0 & 0 & 0 & \frac{12EI_y}{L^3(1+\phi_z)} & & & \\
0 & 0 & 0 & \frac{-GJ}{L} & 0 & 0 & 0 & 0 & 0 & \frac{GJ}{L} & & \\
0 & 0 & \frac{-6EI_y}{L^2(1+\phi_z)} & 0 & \frac{(2-\phi_z)EI_y}{L(1+\phi_z)} & 0 & 0 & 0 & \frac{6EI_y}{L^2(1+\phi_z)} & 0 & \frac{(4+\phi_z)EI_y}{L(1+\phi_z)} & \\
0 & \frac{6EI_z}{L^2(1+\phi_z)} & 0 & 0 & 0 & \frac{(2-\phi_y)EI_z}{L(1+\phi_y)} & 0 & \frac{-6EI_z}{L^2(1+\phi_y)} & 0 & 0 & 0 & \frac{(4+\phi_y)EI_z}{L(1+\phi_y)}
\end{array}
$$

$D_m \sin w_n t$ = the displacement of the mass point 'm'

M_m = the value of the mass

w_n = natural frequency of the n^{th} mode

A set of such equations may be represented in matrix form :

$$\{P\} = w_n^2 [M] \{D\} \tag{2.4.2}$$

where, M is given by

$$M = \begin{bmatrix} m_1 & & & & & & & & & & & 0 \\ & m_1 & & & & & & & & & & \\ & & m_1 & & & & & & & & & \\ & & & I_{MXX} & & & & & & & & \\ & & & & I_{MYY} & & & & & & & \\ & & & & & I_{MZZ} & & & & & & \\ & & & & & & m_1 & & & & & \\ & & & & & & & m_1 & & & & \\ & & & & & & & & m_1 & & & \\ & & & & & & & & & I_{MXX} & & \\ & & & & & & & & & & I_{MYY} & \\ 0 & & & & & & & & & & & I_{MZZ} \end{bmatrix}$$

Where, m_1 = mass of half the element

I_{MXX}, I_{MYY}, I_{MZZ} are mass moments of inertia of half the element about the specified axes.

2.5 ROTATION TRANSFORMATION MATRIX

The element stiffness matrix is formulated first for element oriented axes. It is necessary to obtain element stiffness-matrix in the structure axes

with a view to assemble all element-stiffness matrices to produce the structure stiffness matrix.

The element-stiffness-matrix in the structure axes is obtained from element-stiffness-matrix in element axes, by method of rotation of axes. The rotation transformation[9] matrix corresponds to the 12 types of displacements in the direction of structure axes.

In general, the space frame element may have its principal axes y_e and z_e in skew directions. The orientation of the principal axes is specified by means of an angle (θ) of rotation about the x_e-axis. Such an angle is measured by considering the three successive rotations from structure axes to the element axes (Fig. 7 and 8).

R_β (3x3) rotation matrix for rotation about Y_s axis is given by

$$R_\beta = \begin{bmatrix} \cos\beta & 0 & \sin\beta \\ 0 & 1 & 0 \\ -\sin\beta & 0 & \cos\beta \end{bmatrix} \qquad (2.5.1)$$

R_γ (3x3) rotation matrix for rotation about Z_β axis is given by

$$R_\gamma = \begin{bmatrix} \cos\gamma & \sin\gamma & 0 \\ -\sin\gamma & \cos\gamma & 0 \\ 0 & 0 & 1 \end{bmatrix} \qquad (2.5.2)$$

R_θ (3x3) rotation matrix for rotation about x_c-axis is given by

$$R_\theta = \begin{bmatrix} 1 & 0 & 0 \\ 0 & \text{Cos}\,\theta & \text{Sin}\,\theta \\ 0 & -\text{Sin}\,\theta & \text{Cos}\,\theta \end{bmatrix} \tag{2.5.3}$$

The rotation matrix for the three successive rotations shown in Fig. 7 is given by

$$R = R_\theta \; R_\beta \; R_\gamma \tag{2.5.4}$$

In terms of direction cosines,

$$R = \begin{bmatrix} C_x & C_y & C_z \\ \dfrac{-C_xC_y\text{Cos}\,\theta \;\; -C_z\text{Sin}\,\theta}{\sqrt{C_x^2 + C_z^2}} & \sqrt{C_x^2 + C_z^2}\;\text{Cos}\,\theta & \dfrac{-C_yC_z\text{Cos}\,\theta + C_x\text{Sin}\,\theta}{\sqrt{C_x^2 + C_z^2}} \\ \dfrac{C_xC_y\text{Sin}\,\theta - C_z\text{Cos}\,\theta}{\sqrt{C_x^2 + C_z^2}} & \sqrt{C_x^2 + C_z^2}\;\text{Sin}\,\theta & \dfrac{C_yC_z\text{Sin}\,\theta + C_x\text{Cos}\,\theta}{\sqrt{C_x^2 + C_z^2}} \end{bmatrix} \tag{2.5.5}$$

The direction cosines are calculated from the coordinates of the joints.

The rotation transformation matrix R_T for a space frame element is given by,

$$R_T = \begin{bmatrix} R & 0 & 0 & 0 \\ 0 & R & 0 & 0 \\ 0 & 0 & R & 0 \\ 0 & 0 & 0 & R \end{bmatrix} \tag{2.5.6}$$

For a vertical member, the rotation transformation matrix is given by,

$$R_T = \begin{bmatrix} 0 & C_y & 0 \\ -C_y \cos\theta & 0 & \sin\theta \\ C_y \sin\theta & 0 & \cos\theta \end{bmatrix} \qquad (2.5.7)$$

If K_E = Element Stiffness-matrix in element oriented axes

K_{ED} = Element Stiffness-matrix in structure axes

then

$$K_{ED} = R_T^1 \, K_E \, R_T \qquad (2.5.8)$$

where

R_T^1 is the transpose of R_T.

Similarly,

$$AM = R_T^1 \, EM \, R_T \qquad (2.5.9)$$

where

EM = Element mass matrix in element oriented axes

AM = Element mass matrix in structure axes.

2.6 STRUCTURE STIFFNESS MATRIX

A member 'i' in a space frame will have joint numbers j and k at its ends. There are twelve displacements of the joints associated with this member.

The (12x12) stiffness-matrix K_{ED} is generated for each element (Art 2.3) and its contributions to the stiffnesses of joints j and k are assessed. For

example the first column in matrix K_{ED} contributes to the over-all joint stiffness matrix[9] K_J as follows :

$$
\begin{aligned}
(K_J)_{j1,j1} &= \sum K_{ED} + (K_{ED1,1})_i \\
(K_J)_{j2,j1} &= \sum K_{ED} + (K_{ED2,1})_i \\
(K_J)_{j3,j1} &= \sum K_{ED} + (K_{ED3,1})_i \\
(K_J)_{j4,j1} &= \sum K_{ED} + (K_{ED4,1})_i \\
(K_J)_{j5,j1} &= \sum K_{ED} + (K_{ED5,1})_i \\
(K_J)_{j6,j1} &= \sum K_{ED} + (K_{ED6,1})_i \\
(K_J)_{k1,j1} &= (K_{ED7,1})_i \\
(K_J)_{k2,j1} &= (K_{ED8,1})_i \\
(K_J)_{k3,j1} &= (K_{ED9,1})_i \\
(K_J)_{k4,j1} &= (K_{ED10,1})_i \\
(K_J)_{k5,j1} &= (K_{ED11,1})_i \\
(K_J)_{k6,j1} &= (K_{ED12,1})_i
\end{aligned}
\qquad (2.6.1)
$$

The first subscript of (K_J) is the number that denotes the location of the action itself and the second is the index for the unit displacement causing the action. $\sum K_{ED}$ is the contribution of all other elements forming the joint. Eleven other sets of

equations. Each set involves transferring elements from a given column in the matrix K_{ED} to the appropriate locations in the matrix (K_J).

The structural mass matrix is obtained in exactly the same way. The element mass matrix in global coordinates is generated. The contribution of each element forming the joint is assessed and posted to the appropriate locations in the over-all structural mass matrix which is a diagonal matrix in the present formulation.

2.7 SECTIONAL PROPERTIES

Elastic and inertia properties of the elements constituting the structure, must be known to construct the stiffness and mass matrices of the elements. These properties are evaluated using the sectional properties of the element. The sectional properties needed are 1) area, 2) the location of centre of area, 3) the principal axes through the centre of area and 4) the second moments of area with respect to the principal axes.

The method enumerated in reference (11) is used to determine the required sectional properties. The contour of each section is approximated by a sequence of straight lines and circular arcs which are convex or concave. A set of suitable local axes is chosen, with respect to which, coordinates of each segment of the contour are stated. The contour of the section is

divided into two portions, upper and lower, between two extreme corners. Sectional properties are calculated for both upper lower portion segments. Summing up the respective properties for all the upper and lower portion segments, the properties of the section in question are found as the difference between the sums. The co-ordinates of the centre of area are found by dividing the appropriate first moments of area by the area of the cross-section.

The principal second moments of area are found by transferring the second moments of area I_x, I_y, I_{xy}, calculated in local axes, to a system of co-ordinate axes (x', y') parallel to the local axes and passing through the centre of area and then rotating the (x', y') axes through an angle θ given by

$$\theta = \frac{1}{2} \tan^{-1} \frac{2 I_{x'y'}}{I_{y'} - I_{x'}} \qquad (2.7.1)$$

θ is measured from x'-axis and it is taken as positive in the anti-clockwise direction. The principal second moments of area are evaluated from the expressions;

$$\begin{aligned} I_{x''} &= I_{x'} \cos^2 \theta + I_{y'} \sin^2 \theta - I_{x'y'} \sin 2\theta \\ I_{y''} &= I_{x'} \sin^2 \theta + I_{y'} \cos^2 \theta + I_{x'y'} \sin 2\theta \end{aligned} \qquad (2.7.2)$$

2.8 INERTIA PROPERTIES

m_1 = mass of half the element

$$= \frac{1}{2} \rho AL \qquad (2.8.1)$$

where ρ = mass density of the material

A = area of cross-section of the element

L = length of the element

I_{MXX} = mass moment of inertia about x-axis

$$= \rho \int_V (z^2 + y^2)\, dx\, dy\, dz = \frac{\rho L}{2} (I_y + I_z) \qquad (2.8.2)$$

where V = volume of half the element

I_{MYY} = mass moment of inertia about y-axis

$$= \rho \int_V (z^2 + x^2)\, dx\, dy\, dz = \rho \left[\frac{AL^3}{24} + \frac{I_y L}{2}\right] \qquad (2.8.3)$$

I_{MZZ} = mass moment of inertia about z-axis

$$= \rho \int_V (x^2 + y^2) dx\, dy\, dz = \rho \left[\frac{AL^3}{24} + \frac{I_z L}{2}\right] \qquad (2.8.4)$$

The x, y and z axes are element oriented axes.

2.9 DERIVATION OF NATURAL FREQUENCY

The equations[13] of motion for multi-degree lumped-mass system may be written as

$$\left[M\right]_D \{\ddot{y}\} + \left[K\right]\{Y\} = \{F(t)\} \qquad (2.9.1)$$

where

$\left[M\right]_D$ = diagonal matrix containing masses of the system

$\{y\}$, $\{\ddot{y}\}$ = the generalized co-ordinates and their second derivatives respectively

$[K]$ = square stiffness matrix

$\{F(t)\}$ = a column matrix of applied forces

If the system is vibrating in a normal mode we may make the substitutions,

$$\{y\} = \{a_n\} \operatorname{Sin} w_n t, \; \{\ddot{y}\} = - w_n^2 \; \{a_n\} \operatorname{Sin} \; w_n t$$
$$\{F(t)\} = 0$$

to obtain

$$- w_n^2 \, [M]_D \, \{a_n\} + [K]\{a_n\} = 0$$

or
$$(K - w_n^2 \; M_D) \, \{a_n\} = 0 \tag{2.9.2}$$

where $\{a_n\}$ is the column matrix or vector, of the modal displacements for the n^{th} mode. Noting that a_n cannot be zero and using Cramer's rule, we write

$$\left| [K] - w_n^2 \, [M]_D \right| = 0 \tag{2.9.3}$$

Premultiplying equation (2.9.3) by $[K]^{-1}$ we get

$$\left| I - w_n^2 \, [K]^{-1} \, [M]_D \right| = 0 \tag{2.9.4}$$

$$\left| \frac{1}{w_n^2} \; I - [K]^{-1} \, [M]_D \right| = 0 \tag{2.9.5}$$

Substituting $\lambda = \frac{1}{w_n^2}$

$$\left| \lambda I - [K]^{-1} [M]_D \right| = 0 \tag{2.9.6}$$

$[K]^{-1} [M]_D$ is called the dynamic matrix.

Designating this matrix by A, we get

$$\left| A - \lambda I \right| = 0 \tag{2.9.7}$$

Eigen value λ gives the reciprocal of the square of the natural frequency. Associated with each eigen value λ is an eigen vector giving the characteristic mode shape. The dynamic matrix

$$A = [K]^{-1} [M]_D$$

is non-symmetric. Therefore power method[14] is used to obtain the solution of equation (2.9.7).

CHAPTER III

EFFECT OF STRUCTURAL PARAMETERS ON NATURAL FREQUENCY

The thickness 't' and depth 'd' of the front and rear walls are varied to study the effect of these parameters on the natural frequency of the lathe-bed. The sectional details of the ribs are kept the same as given in the original drawing.

For idealization shown in Fig. 2, first six natural frequencies are computed for five combinations of 't' and 'd'. For the design under consideration (HMT Lathe-bed, SK-62-206-5, Appendix II) t = 2.5 cm and over all depth d = 38.0 cm. The thickness is varied from 1.5 cm to 3.5 cm in steps of 5 mm. In each case the depth is suitably chosen such that the mass of the bed is very nearly constant. The maximum variation of the mass in the present case is found to be about 1.4%. Length and width of the bed are held constant.

The natural frequencies for the above variations are given in Table 2. The computed results are also plotted in Fig. 13, with natural frequency as ordinate and thickness to depth ratio as abscissa. It is seen that for the first mode the t/d ratio of 0.0658 gives the highest natural frequency. For the rest of

the modes it is clear that the natural frequency rises rather steeply with increase in t/d ratio and it reaches its maximum value in the neighbourhood of t/d=0.09. The curves of Fig.13 do not represent exact or empirical mathematical relationship between natural frequency and t/d ratio. However, they give an idea of probable variation of natural frequency with t/d ratio. The changes in natural frequency for each change in the parameters 't' and 'd' can be readily assessed when the natural frequency is an important criterion of design.

An alternative idealization is shown in Fig.9. In this case, the elements 9, 10, 18, 17, 14 and 11, 12, 20, 19, 15 as shown in Fig. 2 are replaced by two inverted 'U' shaped elements. The idealization has 48 degrees of freedom. The first fundamental natural frequency is 129.5 CPS. This is about 9.2% less than that produced by the previous idealization. The time required for processing this programme in IBM7044 computer is a little over 3 minutes. On the other hand the programme of the more detailed idealization with 108 d.o.f takes more than 22 minutes. Therefore for the purposes of an estimation the idealization with 48 d.o.f (Fig. 9) is well suited.

The first three mode shapes, for idealization (Fig. 2) with t=2.5 cm and d=38.0 cm are shown in Fig. 10, 11 and 12.

TABLE 2

Computed Natural Frequencies in cps.

	Idealization I. Fig. 2 D.O.F = 108					Idealization II Fig.9 D.O.F=48
t cm	1.5	2.0	2.5	3.0	3.5	2.5
d cm	56.8	45.1	38.0	33.3	29.9	38.0
Mode	Natural Frequencies in cps.					
1	131.5	128.5	141.0	134.0	135.4	129.5
2	184.0	228.0	279.0	278.0	270.0	243.0
3	206.0	269.0	283.0	290.0	289.0	272.0
4	239.0	276.0	291.0	297.0	294.0	343.0
5	260.0	286.0	299.0	305.0	298.0	540.0
6	263.0	295.0	306.0	308.0	307.0	663.0

Natural frequency values are rounded-off for clarity of comparison.

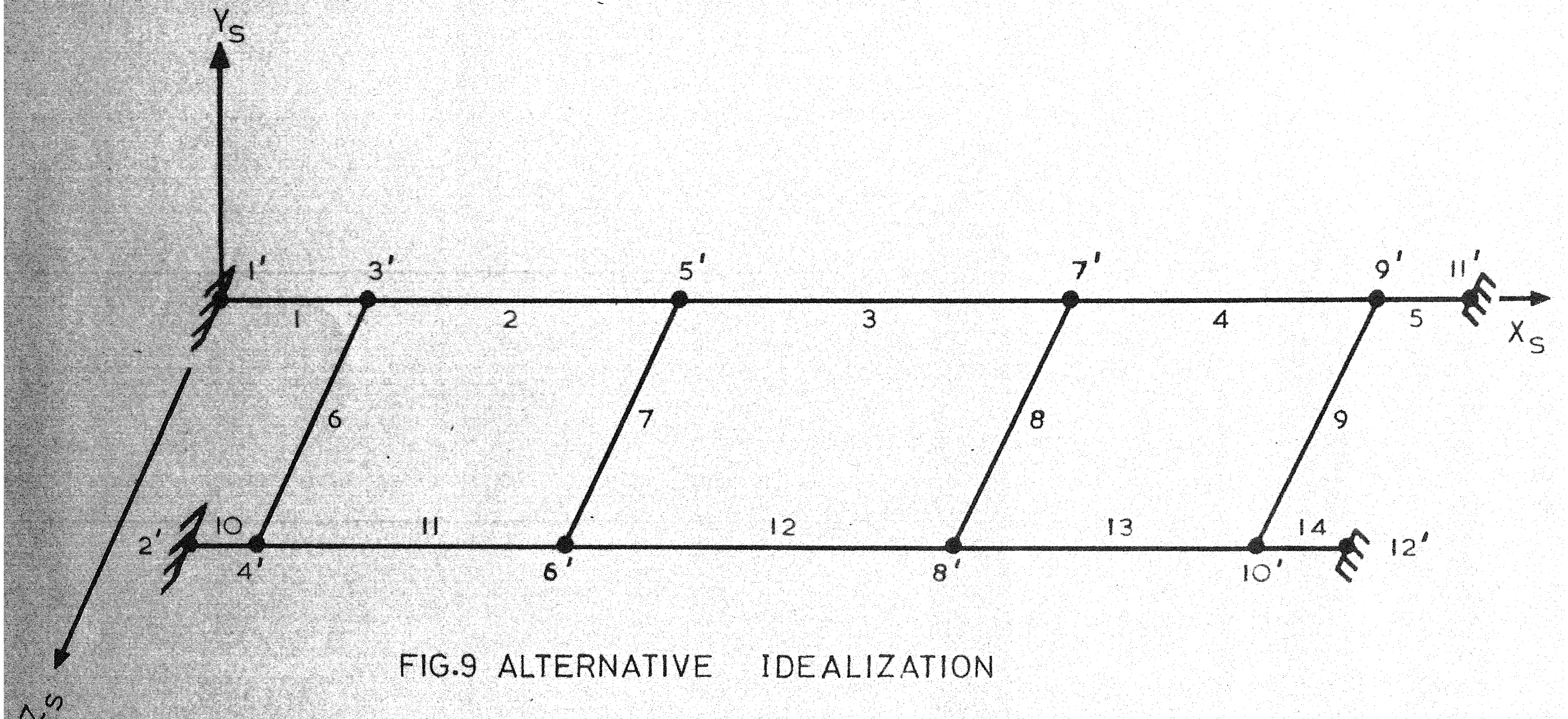

FIG.9 ALTERNATIVE IDEALIZATION

No. of elements 14

No. of joints 12 (primed numbers)

No. of restrained joints 4

No. of freedom 48

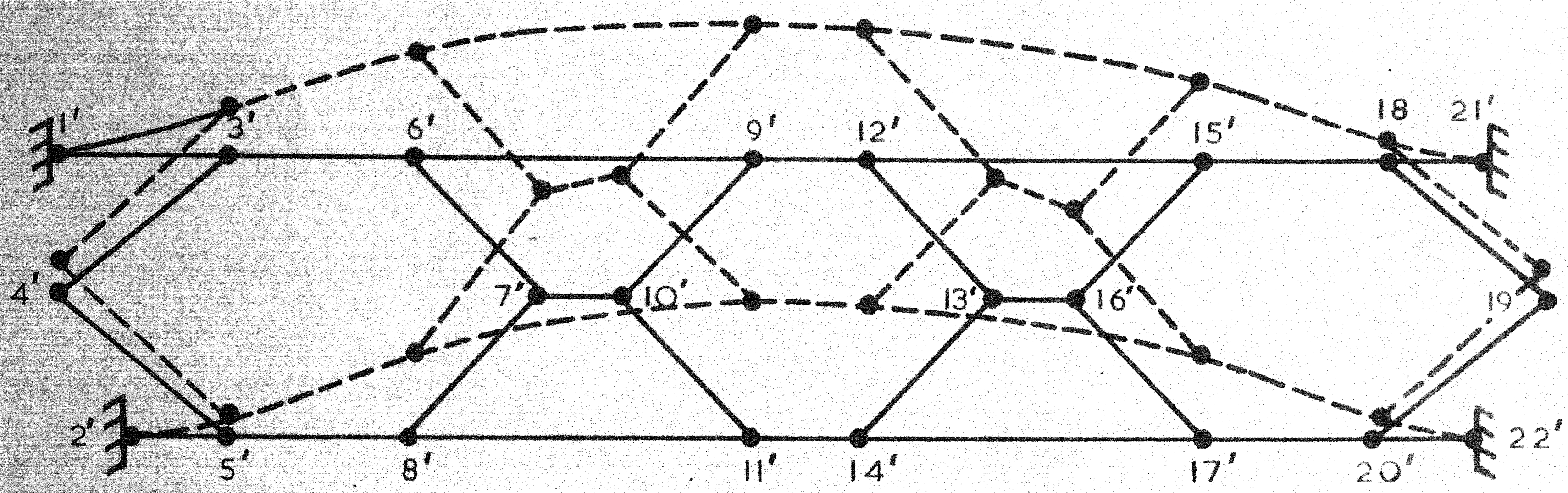

FIG. 10 MODE SHAPE

1st MODE, NATURAL FREQUENCY 141 C.P.S.
(LATERAL VIBRATION)

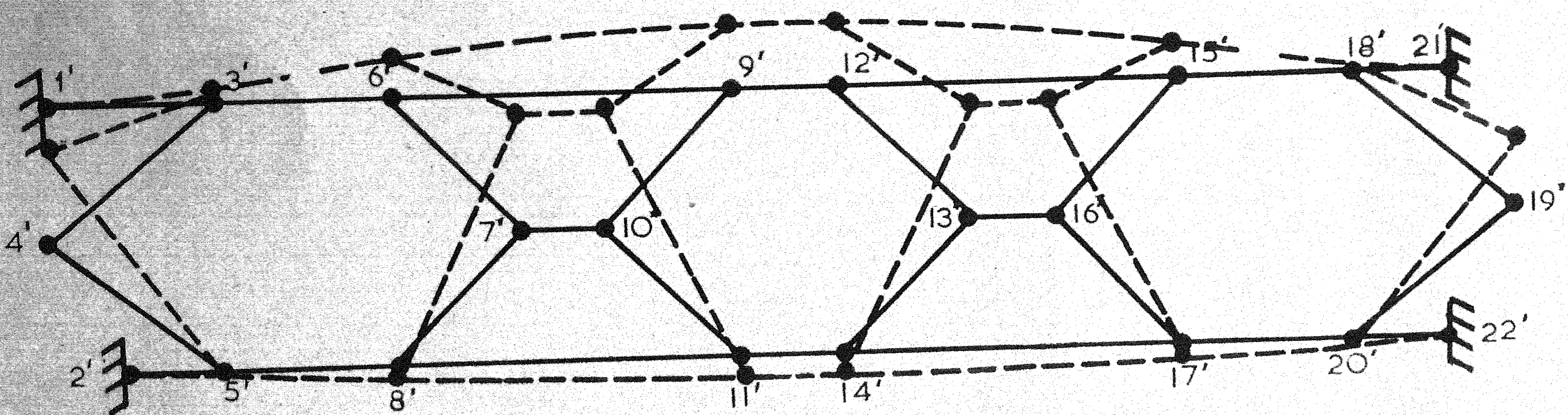

FIG. 11 MODE SHAPE

IInd MODE, NATURAL FREQUENCY 279 CPS
(TORSIONAL VIBRATION)

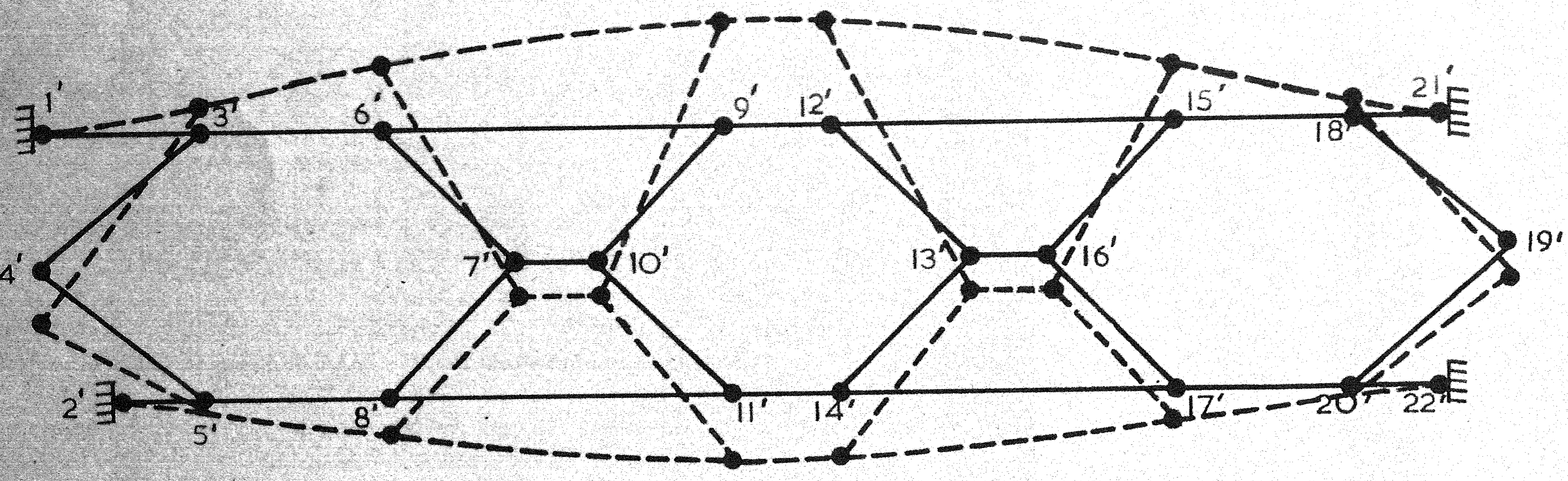

FIG. 12 MODE SHAPE

III rd MODE, NATURAL FREQUENCY
283 C.P.S.
(TORSIONAL VIBRATION)

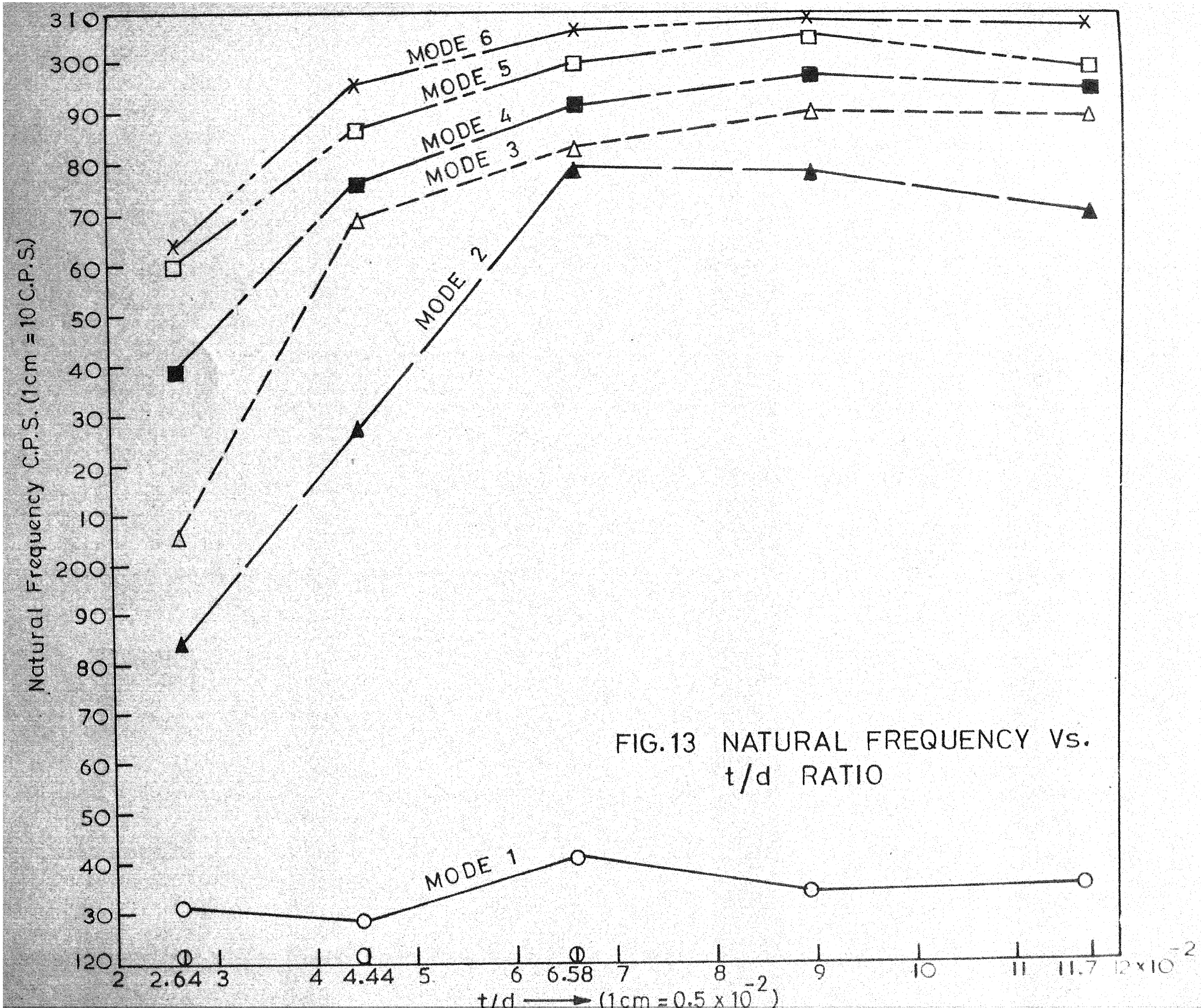

FIG. 13 NATURAL FREQUENCY Vs. t/d RATIO

CHAPTER IV

CONCLUSIONS AND SUGGESTIONS FOR FUTURE WORK

Conclusions :

1) The highest first-fundamental natural frequency occurs at $t/d = 0.0658$. This t/d ratio, incidentally, happens to be the ratio for the design under investigation. As the highest magnitude of the first-fundamental natural frequency is desirable, the design is satisfactory from this point of view for the conditions stipulated.

2) The computer programme developed is a general one. It can be used by designers to study the effects of variation in structural parameters. It can also be used to analyze lathe-bed structure with different types of ribbings for predicting natural frequencies and modes of vibration.

Suggestion for future work :

Width 'w' of the bed, in combination with 't' or 'd' may be varied and changes in natural frequency may be assessed.

To overcome some of the objections to modelling based on beam-like element approach, the elements may be treated as plates and finite-element method may be used for the analysis.

REFERENCES

1. TOBIAS, S.A., Machine Tool Vibrations, Blackie, 1965.

2. ANDREW, C. AND TOBIAS, S.A., A Critical Comparison of Two Current Theories of Machine Tool Chatter, International Journal of M.T.D.R. Vol. I, 1961, pp 325.

3. HAHN, R.S., On Theory of Regenerative Chatter in Precision Grinding Operations, Trans. ASME, Vol.76, 1954, pp 593.

4. KOENIGSBERGER, F. AND TLUSTY, J., Machine Tool Structures, Pergamon Press, 1970.

5. TAYLOR, S. AND TOBIAS, S.A., Lumped-Constant Method for Prediction of Vibration Characteristics of Machine Tool Structures, Advances in Machine Tool Design and Research, September, 1964, pp 37.

6. TAYLOR, S., A Computer Analysis of Open Side Planning Machine, Advances in Machine Tool Design and Research, September, 1965, pp 197.

7. TAYLOR, S. AND TOBIAS, S.A., Computer Methods for the Structural Analysis of Machine Tools, Annals of C.I.R.P., Pergamon Press, 1969.

8. HINDUJA, S. AND COWLEY, A., The Finite-element Method Applied to the Deformation Analysis of the Thin-walled Columns, Machine Tool Design and Research, Vol. 12, 1972, pp 455, 475.

9. GERE, J.M. AND WEAVER, W., Analysis of Framed Structures, East-West Press, 1969.

10. PRZEMIENIECKI, J.S., Theory of Matrix Structural Analysis, McGraw-Hill Book Co., 1968.

11. MALTBACK, J.C., Moments of Area of Aerofoil Sections, Aircraft Engineering, Vol. 33, December, 1961.

12. GUPTA, A.K., Investigation into Dynamic Response of a Lathe-bed, M.Tech. Thesis, I.I.T. Kanpur, August, 1970.

13. JOHN, M. BIGGS, Introduction to Structural Dynamics, McGraw-Hill Book Co., 1964.

14. BRICE CARNAHAN, H.A. LUTHER AND JAMES, O. WILKES, Applied Numerical Methods, John Wiley and Sons, Inc. 1969.

15. HURTY, W.C. AND RUBINSTEIN, M.F., Dynamics of Structures, Prentice Hall of India, 1967.

APPENDIX I

COMPUTER PROGRAMME FLOW DIAGRAM